HMM-based Pathological Gait Analyzer for a User-Adaptive Intelligent Robotic Walker

Georgia Chalvatzaki, Xanthi S. Papageorgiou, Costas S. Tzafestas and Petros Maragos
School of Electrical and Computer Engineering, National Technical University of Athens, Greece
{gchal,xpapag}@mail.ntua.gr, {ktzaf,maragos}@cs.ntua.gr

***Abstract*— During the past decade, robotic technology has evolved considerably towards the development of cognitive robotic systems that enable close interaction with humans. Application fields of such novel robotic technologies are now wide spreading covering a variety of human assistance functionalities, aiming in particular at supporting the needs of human beings experiencing various forms of mobility or cognitive impairments. Mobility impairments are prevalent in the elderly population and constitute one of the main causes related to difficulties in performing Activities of Daily Living (ADLs) and consequent reduction of quality of life. This paper reports current research work related to the development of a pathological gait analyzer for intelligent robotic rollator aiming to be an input to a user-adaptive and context-aware robot control architecture. Specifically, we present a novel method for human leg tracking using Particle Filters and Probablistic Data Association from a laser scanner, constituting a non-wearable and non-intrusive approach. The tracked positions and velocities of the user's legs are the observables of an HMM, which provides the gait phases of the detected gait cycles. Given those phases we compute specific gait parameters, which are used for medical diagnosis. The results of our pathological gait analyzer are validated using ground truth data from a GAITRite system. The results presented in this paper demonstrate that the proposed human data analysis scheme has the potential to provide the necessary methodological (modeling, inference, and learning) framework for a cognitive behavior-based robot control system.**

I. INTRODUCTION

Elder care constitutes a major issue for modern societies, as the elderly population constantly increases [1]. Mobility problems are common in seniors. As people age they have to cope with instability and lower walking speed [2]. It is well known that mobility impairments constitute a key factor impeding many activities of daily living important to independent living, having a strong impact in productive life, independence, physical exercise, and self-esteem [3], [4]. Medical experts commonly use the Performance-Oriented Mobility Assessment (**POMA**) tool to assess the mobility status of patients, [5], in order to propose a proper rehabilitation treatment. It is known that certain pathologies are responsible for changes in stride length and alterations in phases of walking [6], while it seems that basic gait parameters of normal subjects are affected with aging [7]. Medical studies for past-stroke patients establish the significance of evaluating the gait parameters for rehabilitation purposes [8].

This research work has been partially supported by two EU-funded Projects: BabyRobot (H2020, grant agreement no. 687831) and I-SUPPORT (H2020-PHC-19-2014, grant agreement no. 643666).

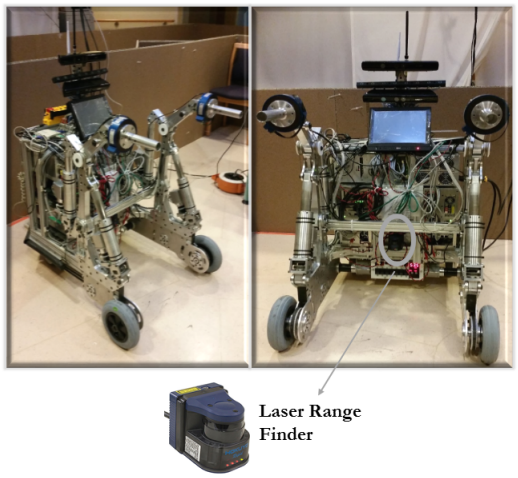

Fig. 1: Left: Typical passive assistive device for elderly. Right: The robotic platform based on the rollator prototype equipped with a Hokuyo Laser Sensor aiming to record user's gait data.

Most people with mobility issues, patients or elders, have to use walkers in their everyday activities and they need the constant supervision of a carer. The social and economic significance of solving these issue should not be underestimated. Robotics seems to fit naturally to the role of assistance since it can incorporate features such as posture support and stability enhancement, walking assistance, navigation and cognitive assistance in indoor and outdoor environments, health monitoring etc.

This paper reports research work conducted in the frames of an EU funded research project MOBOT, aiming to develop an intelligent robotic rollator aiming to provide user-adaptive and context-aware walking assistance (see Fig. 1). The main motivation behind this work derives from our vision of developing and advancing robotic technologies enabling the development and deployment of cognitive assistive devices that can monitor and understand specific forms of human walking activities in their workspace, in order to deduce the particular needs of a user regarding mobility and ambulation. The ultimate goal is to provide context-aware support [9], and intuitive, user-adapted assistance to users experiencing

mild to moderate mobility and/or cognitive impairments in domestic environments. To achieve such targets, a large spectrum of multimodal sensory processing and interactive control modules need to be developed and seamlessly integrated, that can, on one side track and analyse human motions and actions, in order to detect pathological situations and estimate user needs, while predicting at the same time the user (short-term or long-range) intentions in order to adapt robot control actions and supportive behaviours accordingly. User-oriented human-robot interaction and control refers to the functionalities that couple the motions, the actions and, in more general terms, the behaviours of the assistive robotic device to the user in a *non-physical interaction* context.

In this paper, we summarise current research work, focusing on recent advances and challenges regarding the development of a reliable pathological walking assessment system, that can operate on-line and in real-time enabling the robotic assistive device to continuously monitor and analyse the gait characteristics of the user in order to recognise walking patterns that can be classified as pathological requiring specific attention and handling by the system. The proposed system uses an onboard laser rangefinder sensor to detect the user legs which are tracked using Particle Filters with a Probabilistic Data Association framework (PDA-PF) (a non-intrusive solution that does not interfere with human motion). A hidden Markov model (HMM) approach is used to perform statistical modeling of human gait. This paper presents the results of this gait modeling framework in terms of segmenting the gait cycle and recognising different gait phases, which can be subsequently used to extract gait parameters. These parameters are commonly used for medical diagnosis. This paper presents preliminary gait characterisation results for three patients regarding their POMA score, from a full-scale experimental study conducted at the premises of the Bethanien Hospital - Geriatric Centre of the University of Heidelberg, at the frames of the EU-funded FP7 research project MOBOT.

In this paper, we experimentally validate the affect of custom-made control designs on the patient's walking performance, relative to his medical categorization (POMA score), through the estimation of appropriate gait parameters. In this first study, we show that patients of different mobility state (different POMA scores) do not always benefit from a generic control setting of the mobility device. The results of this study provide sufficient first evidence that a robotic personal assistant should be user-adaptive, justifying the necessity for a context-aware robot control architecture that will take feedback from our in-house developed system for real-time gait status estimation. This paper summarizes the theoretical framework and presents current experimental results obtained using real data both from patients (elderly subjects with mild to moderate walking impairments) and normal subjects. With respect to gait analysis and assessment, as opposed to most of the literature available on the topic, the approach presented in this paper is completely non-intrusive based on the use of a typical non-wearable device. Instead of using complex models and motion tracking approaches that require expensive or bulky sensors and recording devices that interfere with human motion, the measured data used in this work is provided by a standard laser rangefinder sensor mounted on the prototype robotic rollator platform. In this paper, we perform an initial assessment of an HMM-based methodology used for the statistical modeling and classification of human gait patterns and for the extraction of clinically-relevant gait parameters and we elaborate on the capability of the system to discriminate the different classes of pathological gait regarding to the patients' POMA score.

Fig. 2: Internal gait phases of human normal gait cycle.

The experimental results presented in this paper are promising, demonstrating that such a framework can be used efficiently and effectively to provide user-adapted mobility assistance that can enhance the functionality of such robotic devices. The ultimate objective of this work is to design a reliable pathological walking assessment system (that embodies several walking morphologies, allowing inclusion of new patients with different mobility pathologies) and incorporate this tracking and monitoring system in a context-aware robot control framework enabling a cognitive mobility assistance robotic device to provide user-adaptive walking support actions and intuitive assistive behaviours.

The paper is organised as follows. Section II presents a general description of the context-aware robot control we designed. The normal human gait cycle is described in Section III and Section IV describes the proposed HMM-based gait analysis and characterisation framework. Section V describes the experimental results achieved regarding the gait analysis, providing also validation results using data from a GAITRite mat while Section VI presents conclusions and summarises future research work directions.

II. USER-ADAPTIVE CONTEXT-AWARE ROBOT CONTROL ARCHITECTURE

An Adaptive Context-Aware Robot Control architecture is being developed for the intelligent robotic assistant platform, that will adapt and act according to the patient's needs. The system is driven by the sensory data of a 2D laser range

scanner that detects the walking motion (Fig.1). An important step for performing behavior-based context aware control is the preprocessing of the system's input signal. This process incorporates the detection and tracking of the user's legs. This framework takes as input the noisy laser data, detects the patient's legs and estimates their actual position and velocity with respect to the robotic assistant. The estimated kinematic state of the subject's legs feed the cognitive context-aware control system as the environmental input signal, that is used to infer the context (i.e. state of the patient) and to perform specific actions in the detected context.

The control scheme consists of the typical three-layer architecture. The high level of this control scheme contains the Gait Modelling and Classification module. This is an HMM-based approach that can recognize sequences of gait patterns and also it can classify them into normal pathological ones, or non-walking activity. Given the spatiotemporal properties of those sequences, we compute particular gait parameters (such as step length, cadence), that are commonly used for medical diagnosis [10], since differentiations in their values are indicative of specific pathological states. In that way, an impairment level assessment is performed, for completely knowing the context of the patient's walking motion (i.e. recognition of the patient's intention to walk, gait modelling, estimation of the subject's pathological status).

This context-awareness is used as input to the medium level control module. Medium level control contains specific behaviours and assistive actions, that are activated according to the subject's detected context. The robotic assistant should adaptively track and follow the subject during its walking motion. Also the platform should smoothly stop in front of the subject in cases when the subject freezes and stops abruptly. Furthermore, the platform should smoothly approach the user to provide possible support when instability in gaiting is detected.

All this information is used as input to the typical low level controller of the platform, in order to inherently translate the decision of performing a specific assistive action into motor commands.

III. HUMAN GAIT CYCLE ANALYSIS

The human gait motion analysis is based on the periodic movement of each foot from one position of support to the next [11]. There are two main periods in the gait cycle [12]: The stance, when the foot is on the ground, and the swing when that same foot is no longer in contact with the ground and is swinging through, in preparation for the next foot strike. The gait cycle can be successively divided into eight events, Fig. 2. This segmentation is sufficiently general to be applied to most types of human gait, including five during stance phase and three during swing, which are (as a percentage of the total duration of the gait cycle): 1. **Initial contact** (0%) - **[IC]** -Heel strike initiates the gait cycle and represents the point at which the body's centre of gravity is at its lowest position. 2. **Loading response** (0-10%) - **[LR]** - Foot-flat is the time when the plantar surface of the foot touches the ground. 3. **Midstance** (10-30%) - **[MS]** - Midstance occurs when the swinging (contralateral) foot passes the stance foot and the body's centre of gravity is at its highest position. 4. **Terminal stance** (30-50%) - **[TS]** - Heel-off occurs as the heel loses contact with the ground and pushoff is initiated via the triceps muscles, which plantar flex the ankle. 5. **Preswing** (50-60%) - **[PW]** - Toe-off terminates the stance phase as the foot leaves the ground. 6. **Initial Swing** (60-70%) - **[IW]** - Acceleration begins as soon as the foot leaves the ground and the subject activates the hip flexor muscles to accelerate the leg forward. 7. **Midswing** (70-85%) - **[MW]** - Midswing occurs when the foot passes directly beneath the body, coincidental with midstance for the other foot. 8. **Terminal swing** (85-100%) - **[TW]** - Deceleration describes the action of the muscles as they slow the leg and stabilize the foot in preparation for the next heel strike. In this paper, we have used the seven gait phases of walking in order to analyze the gait cycle, since the TW phase is an equivalent trigger to the IC phase, and therefore are treated as identical.

Specific gait parameters can be computed, which are commonly used for medical diagnosis [10], [13]. In this work, besides from detecting the sequence of gait events according to Fig. 2, we are also experimentally validating the following temporal gait parameters:

1) ***stride length***: the distance traveled by both feet in a gait cycle
2) ***stride time***: the duration of each gait cycle,
3) ***stance time***: the stance phase duration in one cycle,
4) ***swing time***: the swing phase duration in one cycle,
5) ***gait speed***: the mean walking velocity of all gait cycles.

IV. GAIT PARAMETERS EXTRACTION SYSTEM BASED ON HIDDEN MARKOV MODEL

The sequential estimation of the gait parameters are necessary for the gait status assessment of the user. Those parameters are extracted by employing the raw laser data, provided by the laser sensor mounted on the robotic rollator, Fig. 1. The laser data are the observations of a PDA-PF leg tracking system based on two PFs, which are associated probabilistically. PDA-PF sequentially estimates the relative position and velocity of the patient's legs w.r.t. the robotic rollator. The posterior estimates of the legs' states are fed into an HMM, which recognizes the gait cycles and segments them into the corresponding gait phases [12]. We, then, extract the gait parameters corresponding to each gait cycle [14], [15], which are used for the exploration of the control effect on the users gait status.

A. PDA-PF Leg Tracking

The PF is commonly used for nonlinear filtering problems [16]. The particles represent samples of the posterior density distribution of the state space given some observations. Each particle has a weight that results from the observation likelihood. Our implementation incorporates two filters for estimating the position and velocity of each leg separately and associates them probabilistically.

The particles represent samples of the posterior density distribution of the legs' states $\mathbf{x}_k^{left}$ and $\mathbf{x}_k^{right}$ at each time instant k for the left and right leg respectively. Each state constitutes of the Cartesian position and velocity along the axes. The implementation covers the basic particle filter methodology [16], including initialization, propagation in time,particles' weights update, resampling and posterior estimation.

Initialization:

At the first time instant *k=1*, we initialize a set of N particles for each leg. Let the position of the i^{th} particle, for $i = 1,..,N$, be noted as: $\mathbf{p}_k^{f,i} = [\ x \quad y\ ]$ and its velocity as: $\upsilon_k^{f,i} = [\ \upsilon_x \quad \upsilon_y\ ]$, where $f : \{left, right\}$ is the label of each leg. Then, the particles' states are denoted as:

$$\mathbf{x}_k^{f,i} = [\ \mathbf{p}_k^{f,i} \quad \upsilon_k^{f,i}\ ]^T = [\ x \quad y \quad \upsilon_x \quad \upsilon_y\ ]^T$$

Only for initialization, we implement a detection phase using k-means clustering inside a rectangle observation window, to detect the initial positions of the legs with respect to the robotic rollator and to discriminate the left from the right leg. The particles' positions are initialized to be equal to the detected positions, which are computed via circle fitting on the initially detected left and right leg clusters. We also draw N samples for the legs' velocity from a zero-mean Gaussian Mixture Model (**GMM**) distribution (we consider that both legs are still in front of the rollator for initialization). The particles' weights $\omega_k^{f,i}$ of each leg are initialized equal to: $1/N$, with $i = 1,..,N$. The initial posterior estimate is approximated by the Minimum Mean Square Error:

$$\mathbf{x}_k^f = \sum_{i=1}^{N} \omega_k^{f,i} \cdot \mathbf{x}_k^{f,i} = [\ \mathbf{p}_k^f \quad \upsilon_k^f\ ]^T$$

Particles' Propagation:

At each time frame *k=2,..,T* (where T is the total tracking time) the particles' states are propagated in time using the following motion model. We draw N new velocity samples for the particles of each leg from a GMM of two mixtures. We have trained two GMMs that describe the velocity of the two legs along the axes. Let $\upsilon_k^{f,i}$ be the i^{th} velocity sample drawn the respective GMM at time instant k. Then, the position of the i^{th} particle is propagated in time according to the equation:

$$\mathbf{p}_k^{f,i} = \mathbf{p}_{k-1}^f + \upsilon_k^{f,i} \cdot \Delta t$$

where $\mathbf{p}_{k-1}^f$, is the estimated position vector of each leg for the $k-1$ time frame.

Particles' Weights Update:

The particles' weights have to be updated according to the observations of each time instant k. The observations are the Cartesian positions of the laser points in the sagittal plane. In this implementation, we use an observation window for each leg, which is an experimentally defined rectangular area, centered around each particle, so that every sample $\mathbf{x}_k^{f,i}$ is associated with a different cluster of laser points, $\mathbf{y}_k^{f,i}$. Because the prior distribution is equal to the proposal distribution, the particle weights are equal to the observation likelihood [16]: $\omega_k^{f,i} = p(\mathbf{y}_k^{f,i}|\mathbf{x}_k^{f,i})$.

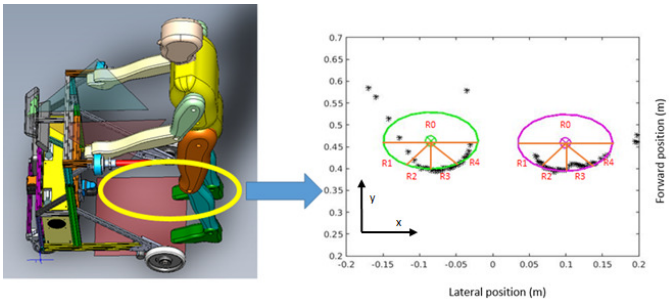

Fig. 3: Example of the circular representation of the legs from the laser points w.r.t. the laser scanner. Left: a cad presentation of a subject walking with the rollator; Right: a presentation of the detected laser points with black stars, with green an magenta are the circular representations of the right and left leg respectively. The labels *R0, R1, R2, R3, R4* are the segmentation of the circle into regions (boundaries depicted with orange lines) based on which we have computed the observation likelihood for the particle filter tracking system.

We treat each particle as a possible leg center and we expect the observations to be on the circular circumference of this center. Thus, the observation likelihood that will provide the weight of the particles is computed based on the following three factors:

1. The distribution of the laser points in the circular contour given the center (i.e. the respective particle): In Fig. 3 an example of the circular representation of the legs from the laser points w.r.t. the laser scanner is presented. On the right of the figure there is a representation of the detected laser points with black stars, while the green and magenta circles are the circular representations of the right and left leg respectively. The labels *R0, R1, R2, R3, R4* represent the segmentation of the circle into regions (the regions' boundaries are depicted with orange lines) based on which we have computed the observation likelihood for the particle filter tracking system. We have divided horizontally the circle into two semicircles. Laser points in the upper semicircle *R0* do not contribute to the observation likelihood. The lower semicircle is split into *four* regions (*R1,..,R4*) of equal angle range. We have calculated the normal distribution of the Euclidean distances of the laser points of each region w.r.t. the corresponding center. Let $\mathbf{d}_{R_m}$ be the vector of distances of the laser points w.r.t. the corresponding circle center for the R_m region, with $m \in 1,...,4$. Thus, each region R_m is described by a normal distribution of the distances $\mathcal{N}(\mathbf{d}_{R_m}|\mu_{R_m}, \Sigma_{R_m})$, with μ_{R_m} the mean distance and Σ_{R_m} is the covariance matrix.

2. The number of laser points inside each observation window: Through experimentation we have defined a normal kernel distribution, noted as λ_i for every particle with $i = 1,..,N$, which describes the likelihood of the number of laser points that are detected on the circular contour that represents the leg.

3. An association probability that accounts the Euclidean distance between the two legs. The human legs are two interacting moving targets, and thus we introduce an association probability β_i, modeled by a Gamma distribution. This probability regulates the observation likelihood of the one leg w.r.t. the other, by evaluating a likelihood of the Euclidean distance of the two legs.

Therefore, every particle is considered to be a possible leg center. We set the observation window centered on the i^{th} particle and we associate it with the corresponding observations, i.e. the laser points $\mathbf{y}_k^{f,i}$ detected inside the window. Then, we consider the i^{th} particle to be a possible leg center and we compute the observation likelihood using the following function:

$$p(\mathbf{y}_k^{f,i}|\mathbf{x}_k^{f,i}) = \beta_i \cdot \left[\lambda_i \cdot \sum_{m=1}^{4} \pi_{R_m} \cdot \prod_{R_m} \mathcal{N}(\mathbf{d}_{R_m}|\mu_{R_m}, \Sigma_{R_m})\right]$$

We assume as π_{R_m}, the importance weights of the four regions, which were set experimentally so that the extreme regions *R1* and *R4*, which often contain many outliers have less importance than the inner regions *R2* and *R3*. All parameters have been experimentally defined. Thus, the i^{th} weight is equal to: $\omega_k^{f,i} = p(\mathbf{y}_k^{f,i}|\mathbf{x}_k^{f,i})$. All weights are normalized for all particles $j = 1,...,N$ according to:

$$\widehat{\omega}_k^{f,i} = \omega_k^{f,i} / \sum_{j=1}^{N} \omega_k^{f,j}$$

Resampling:

It commonly occurs many particles to have infinitely small weight and only a few of the particles will have a significant weight, called weight degeneracy. The solution to this problem is the use of a Sequential Importance Resampling method (SIR) [16], [17], for eliminating particles with small weights and replacing them with particles of higher weights. However, this resampling method illustrates the particle impoverishment problem, where there are many replicates of the higher-likelihood particles, causing the samples to lose their diversity. To deal with this problem, at each time frame we check whether the effective sampling size $N_{eff} = 1/\sum_{i=1}^{N} \widehat{\omega}_k^{f,i}$ is less than the threshold $N_{thr} = N/2$. If so, we apply a random walk on the current particles' state providing new particles ${}^*\mathbf{x}_k^{f,i}$. Then, we evaluate the weights of the new particles, according to the methodology described in Particles' Weights Update section, which provides the new weights: ${}^*\widehat{\omega}_k^{f,i}$. Having the old pairs of particles and their weights $(\mathbf{x}_k^{f,i}, \widehat{\omega}_k^{f,i})$ and the new ones $({}^*\mathbf{x}_k^{f,i}, {}^*\widehat{\omega}_k^{f,i})$, we apply the Metropolis-Hastings algorithm [18]. Based on this algorithm we can decide whether or not we have to replace the i^{th} pair $(\mathbf{x}_k^{f,i}, \widehat{\omega}_k^{f,i})$ with the new samples $({}^*\mathbf{x}_k^{f,i}, {}^*\widehat{\omega}_k^{f,i})$.

Posterior Estimation:

For the posterior state estimate $p(\mathbf{x}_k^f|\mathbf{y}_k^f)$, we find the particle with the highest weight and then collect the "best" particles, i.e. those which have a weight greater or equal than 80% of the maximum weight:

$$s = \arg\max_i [\widehat{\omega}_k^{f,i} \geqslant 0,8 \cdot \max(\widehat{\omega}_k^{f,i})]$$

where s is the index of the "best" particles, i.e. $s \in S \subseteq \{1,...,N\}$. In that way, we have a dynamic system, that leaves out particles that may track outliers and could contaminate the posterior estimation, and therefore provides smoother estimates. The posterior state estimate is then approximated by the weighted mean of the "best" particles:

$$p(\mathbf{x}_k^f|\mathbf{y}_k^f) = \left(\sum_s \mathbf{x}_k^{f,s} \cdot \widehat{\omega}_k^{f,s}\right) \Big/ \left(\sum_s \widehat{\omega}_k^{f,s}\right)$$

TABLE I: Demographics

Subject	1	2	3	4	5	6
Age	89	83	83	71	82	82
Sex	F	F	F	F	F	M
POMA	7	11	19	20	26	27
Falls	yes	yes	yes	yes	yes	yes

Demographics for the subjects that participated in the experiments.

B. HMM Gait Cycle Recognition

We consider seven hidden states according to the seven gait phases of human gait [12], as shown in Fig. 2. These seven phases can define the hidden states of the HMM, which detects the gait cycles [14], [15]. The states of the HMM at time $k = 1,2,...,T$, where T is the total time, are the values of the (hidden) variable $s_k = i \in \mathbf{S}$, for $i = 1,\ldots,7$, where $1 \equiv IC/TW$, $2 \equiv LR$, $3 \equiv MS$, $4 \equiv TS$, $5 \equiv PW$, $6 \equiv IW$, and $7 \equiv MW$. As observables we utilize the posterior estimates of the legs' states provided by the PDA-PF tracking system, i.e. the legs' positions and velocities along the axes and also the distance between the legs. The observation data are modeled using a GMM. This model can provide temporal segmentation of the time sequence of the legs' states (observations), by estimating an optimal gait phases sequence. Following the HMM notation, the transition probability matrix is defined as $A = \{a_{ij}\}$, where $a_{ij} = P[s_{k+1} = j | s_k = i]$, for $1 \leq i, j \leq M$ and M is the number of states, i.e, the (i, j) element of the matrix represents the transition probability from the i^{th} state at a given time step to the j^{th} state at the following time step. In the normal gait cycle the gait phases follow each other sequentially. Thus, a gait cycle HMM is a left-to-right model. This means that the only feasible transitions from a state i will be either to remain in the same state or to jump to a following state. The transition probability matrix, as well as the prior probability vector (i.e. the vector of probabilities π_i of the system being at state i at the initial time t_1), are estimated using the standard and well known Viterbi algorithm [19].

C. Gait Parameters Computation

The recognized segmentation of gait phases is used to compute the gait parameters from the range data. We are

computing the gait parameters: 1) ***stride length***, i.e. the distance traveled by both feet in a gait cycle, 2) ***stride time***: the duration of each recognized gait cycle, 3) ***stance time***: the stance phase duration in one cycle, i.e. the time between the gait phases **IC** and **PW** (Fig. 2), 4) ***swing time***: the time between the gait phases **PW** and the next **IC**, 5) ***gait speed***: results as the velocity through the stride, i.e. it was computed as the ratio of the stride length to the stride time.

These gait parameters are used for the statistical analysis of walking and the potential classification of the gait status of patients with variant POMA scores.

V. EXPERIMENTAL ANALYSIS & RESULTS

A. Experimental setup and data description

The experimental data used in this work were collected in Agaplesion Bethanien Hospital - Geriatric Center. Patients with moderate to mild impairment, according to clinical evaluation of the medical associates, took part in this experiment. The patients were wearing their normal clothes (no need of specific clothing). We have used a Hokuyo rapid laser sensor (UBG-04LX-F01 with mean sampling period of about 28msec and accuracy of 10mm), mounted on the robotic platform of Fig. 1 for the detection of the patients' legs. A GAITRite System was used to collect ground truth data. GAITRite is an electronic mat, of length 4.6 meters, equipped with pressure sensors placed at 1.27 cm each, used for gait analysis. GAITRite provides measurements of the spatial and temporal gait parameters and is commonly used for medical diagnosis [20]. The HMM was trained by using the recorded data from twelve different patients (without any GAITRite recording) [14].

In this work, we present data from six patients with moderate mobility impairment (aged over 65 years old). Each subject walked straight with physical support of the robotic rollator over the walkway defined by the GAITRite mat. The subjects presented mobility impairments with an average POMA score of 18.34 ± 7.99 and high risk of falling, with 100% of the subjects having had fallen once or twice in the last year. Table I provides analytical demographic information about the participants. It can be seen that the subjects have been arranged according to their POMA score. Patients with POMA score $<= 18$ present high risk of falling, while a POMA score between 18 and 23 indicates a moderate risk of falling [21]. The subjects with POMA score over 24 present better mobility performance.

All patients performed the experimental scenarios under appropriate carer's supervision. The subjects were instructed to walk as normally as possible. This results in a different walking speed for each subject, and in different gait parameters.

In Fig. 4, snapshots of a subject are presented, while performing the experimental scenario, captured by the Kinect camera that was also mounted on the robotic rollator (Fig. 1). Also, in Fig. 5 the sequence of the detected footprints by the GAITRite System for the same subject are depicted.

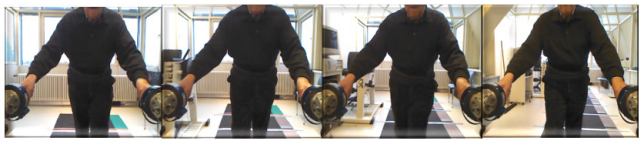

Fig. 4: Snapshots of a subject walking on the GAITRite walkway assisted by the robotic platform, during one stride.

Fig. 5: The captured footprints of the subject by the GAITRite System.

B. Experimental Results and Discussion

For the evaluation of our in-house developed pathological gait analyzer, we present in Table II, the mean values and standard deviations of the gait parameters as those were computed by the HMM-based methodology in contrast to their Ground Truth (**GT**) values. The data are presented in ascending order with respect to the patients' POMA score. The last line of table II presents the Mean Absolute Error (MAE) of the estimated to the ground truth value of each gait parameter. To help us better understand the results of Table II, we present the evolution of the gait parameters w.r.t. the POMA score in the diagrams of Fig. 6. In each diagram, the blue line represents the estimated gait parameters from the HMM-based approach and the red line the ground truth values from the GAITRite system.

Inspecting the results of Table II we can say that regarding the temporal parameters, the time segmentation provided by the HMM-based results are very close to the ground truth values. Regarding, however, the stride length and therefore the gait speed we notice a standard error of the estimated parameter w.r.t. the ground truth provided by the GAITRite system. This results mainly from the fact that the GAITRite system measures the heel to heel distances, while the laser range scanner measures distances approximately at the knee height. Furthermore, the laser scanner measurements depend on the subjects height, and also the movement of the lower limb, the motion of its hypothetical center is not aligned with the heel center movement, making the extraction of the gait parameters even more difficult.

The graphs of Fig. 6 can however show the potential of the HMM-based system to discriminate the different classes of patients, especially regarding the spatial parameter stride length in Fig. 6a and the gait speed in Fig. 6d, where the aforementioned standard error does not seem to affect the behavior of the system, since the evolution of both the stride length and the gait speed w.r.t. the patients' POMA score from the HMM approach follows the same pattern as the graphs of the ground truth data. Fig. 6b and Fig. 6c ascertain the accuracy of the HMM time segmentation, from which we estimate the stride time and stance time, as this is also shown in Table II.

TABLE II: Extracted Gait Parameters

Subject	POMA	Stride Length (m)		Stride Time (s)		Stance Time (s)		Swing Time (s)		Gait Speed (m/s)	
		HMM	GT	HMM	GT	HMM	GT	HMM	GT	HMM	GT
1	7	0.47 ± 0.03	0.58 ± 0.04	1.63 ± 0.05	1.58 ± 0.08	1.00 ± 0.05	0.95 ± 0.10	0.62 ± 0.04	0.63 ± 0.14	0.29 ± 0.02	0.37 ± 0.02
2	11	0.65 ± 0.09	0.79 ± 0.15	1.83 ± 0.07	1.86 ± 0.15	1.08 ± 0.10	1.32 ± 0.21	0.75 ± 0.10	0.54 ± 0.14	0.35 ± 0.06	0.43 ± 0.09
3	19	0.62 ± 0.04	0.7 ± 0.02	1.14 ± 0.03	1.11 ± 0.04	0.71 ± 0.05	0.69 ± 0.04	0.44 ± 0.03	0.42 ± 0.03	0.54 ± 0.04	0.63 ± 0.04
4	20	0.64 ± 0.01	0.77 ± 0.01	1.39 ± 0.01	$1.38 \pm 0/02$	0.91 ± 0.01	0.89 ± 0.03	0.47 ± 0.01	0.48 ± 0.04	0.46 ± 0.01	0.56 ± 0.01
5	26	0.74 ± 0.09	0.94 ± 0.08	1.04 ± 0.04	1.04 ± 0.06	0.68 ± 0.02	0.65 ± 0.02	0.36 ± 0.03	0.39 ± 0.04	0.71 ± 0.06	0.90 ± 0.03
6	27	0.80 ± 0.05	1.02 ± 0.03	1.07 ± 0.02	1.10 ± 0.02	0.66 ± 0.03	0.65 ± 0.01	0.41 ± 0.03	0.45 ± 0.03	0.74 ± 0.06	0.93 ± 0.04
MAE		0.15		0.02		0.06		0.05		0.12	

Gait parameters means and standard deviations computed by the HMM-based along with the ground truth measured parameters of the GAITRite System for the six subjects, along with the MAE for each parameter.

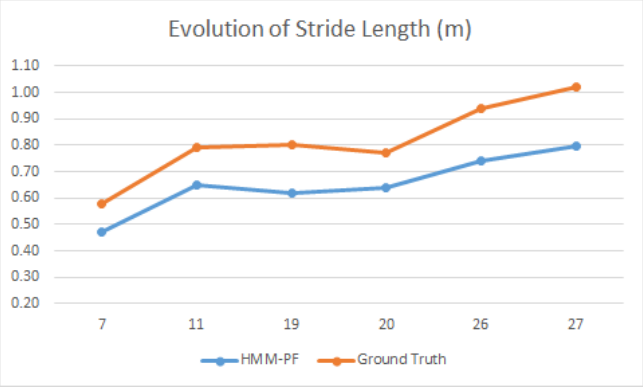

(a) Evolution of the average stride length as it was estimated by the HMM-based system w.r.t. Ground truth data according to the POMA score of the patients.

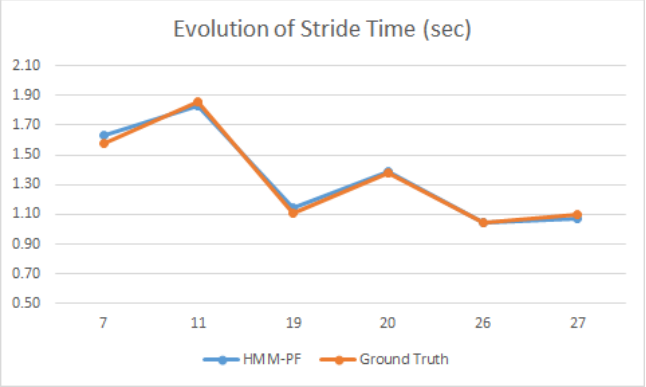

(b) Evolution of the average stride time as it was estimated by the HMM-based system w.r.t. Ground truth data according to the POMA score of the patients.

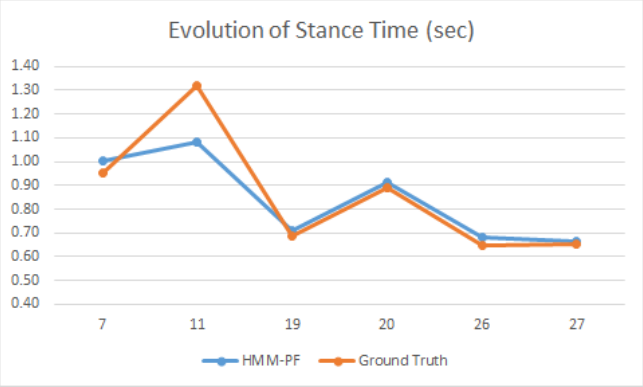

(c) Evolution of the average stance time as it was estimated by the HMM-based system w.r.t. Ground truth data according to the POMA score of the patients.

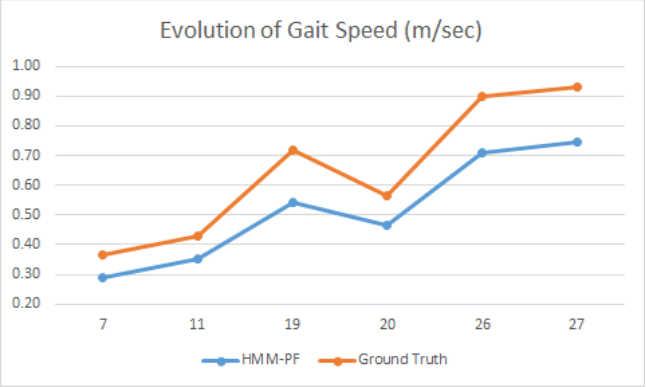

(d) Evolution of the average gait speed as it was estimated by the HMM-based system w.r.t. Ground truth data according to the POMA score of the patients.

Fig. 6: Comparison of the gait parameters evolution regarding their HMM-based estimation and their ground truth values w.r.t. the POMA scores of the participants.

VI. CONCLUSIONS AND FUTURE WORK

The main aim of our research program is the development of a completely non-invasive pathological walking analysis and assessment system, as a subsystem of a context-aware robot control for an intelligent robotic walker. Towards this end, we present current results of our ongoing work regarding the validation study of a human pathological gait analysis and assessment system. Specifically, we test a rule based approach and a Hidden Markov Model (HMM) to recognize the gait phases of the legs and extract specific gait parameters that are used for medical diagnosis. Our system is based on sensor data provided by a typical laser rangefinder sensor, thus constituting a completely non-invasive approach using a non-wearable device. We present a novel approach of human gait tracking using two Particle Filters with probabilistic data association.

Our pathological gait analyzer is validated using ground truth data provided by a GAITRite System, and we provide evidence that our approach can successfully extract the gait parameters in most cases. The experimental results clearly

show that the HMM gait recognition system can be used to provide classification of the users according to their gait parameters. There is significant room for further accuracy increase. Furthermore, the HMM-based approach, because of its statistical learning properties, is quite flexible and readily extensible to different gait models, thus presenting a strong potential to support a behaviour-based cognitive robot control framework. The data presented here are an initial part of a broad ongoing study with more subjects that will be reported upon conclusion of the study. We plan to test different HMM schemes for improved accuracy. As the accuracy of the system is heavily influenced by the training data, we plan to utilize ground truth training data to increase the systems accuracy.

Our main research goal is to use the HMM-based methodology to classify specific gait abnormalities according to pathologies, allowing a variety of abnormal gaits (corresponding to specific motor impairments) to be characterized by different models. Furthermore, within our future plans is to model more gait patterns based on HMM, regarding turning motions during indoor ambulation, as well as more complicated and maneuvering motions that appear in daily activities. We are working to incorporate a more sophisticated detection and tracking system based on particle filtering to cope with these situations. The aim is to create a system that can detect in real time specific gait pathologies and automatically classify the patient status or the rehabilitation progress, thus providing the necessary information for effective cognitive (context-aware) active mobility assistance robots.

REFERENCES

[1] USCensus, "The elderly population," 2010.

[2] T. Herman et. al, "Gait instability and fractal dynamics of older adults with a cautious gait: why do certain older adults walk fearfully?" *Gait Posture 2005*.

[3] P. D. Foundation, "Statistics for parkinson's disease," 2010.

[4] S. Center, "Stroke statistics," 2010.

[5] M. E. Tinetti, "Performance-oriented assessment of mobility problems in elderly patients," *Journal of the American Geriatrics Society 1986*.

[6] J. M. Hausdorff, "Gait dynamics, fractals and falls: Finding meaning in the stride-to-stride fluctuations of human walking," *Human Movement Science 2007*.

[7] T. Oberg et. al., "Basic gait parameters : Reference data for normal subjects, 10-79 years of age," *Journal of Rehabilitation Research and Development*, 1993.

[8] H. von Schroeder et. al, "Gait parameters following stroke: a practical assessment," *Journal of Rehabilitation Research and Development*, 1995.

[9] P. Brezillon, "Context in problem solving: A survey," *The Knowledge Engineering Review*, vol. 14, pp. 1–34, 1999.

[10] A. Muro-de-la-Herran et. al., "Gait analysis methods: An overview of wearable and non-wearable systems, highlighting clinical applications," *Sensors 2014*.

[11] H. Inman et. al., *"Human walking"*. Williams & Wilkins, 1981.

[12] J. Perry, *"Gait Analysis: Normal and Pathological Function"*, 1992.

[13] R. Kressig et. al., "Temporal and spatial features of gait in older adults transitioning to frailty," *Gait Posture 2004*.

[14] X. Papageorgiou et. al., "Hidden markov modeling of human pathological gait using laser range finder for an assisted living intelligent robotic walker," in *IROS 2015*.

[15] X. Papageorgiou et. al, "Experimental validation of human pathological gait analysis for an assisted living intelligent robotic walker," in *Biorob 2016*.

[16] M. Arulampalam et. al., "A tutorial on particle filters for online nonlinear/non-gaussian bayesian tracking," *IEEE Trans. Signal Processing*, 2002.

[17] M. Bolić et. al., "Resampling algorithms for particle filters: A computational complexity perspective," *EURASIP 2014*.

[18] Z. Chen, "Bayesian Filtering: From Kalman Filters to Particle Filters, and Beyond," McMaster University, Tech. Rep., 2003.

[19] L. R. Rabiner, "Readings in speech recognition," A. Waibel and K.-F. Lee, Eds. San Francisco, CA, USA: Morgan Kaufmann Publishers Inc., 1990, ch. A tutorial on hidden Markov models and selected applications in speech recognition, pp. 267–296.

[20] A. Rampp et. al., "Inertial sensor-based stride parameter calculation from gait sequences in geriatric patients," *IEEE Trans. Biomed. Engineering*, 2015.

[21] M. Tinetti, "Fall risk index for elderly patients based on number of chronic disabilities," *The American Journal of Medicine*.